Targeted Covalent Inhibition of Plasmodium FK506 Binding Protein 35

ACS Medicinal Chemistry Letters

pubs.acs.org/acsmedchemlett

Featured Letter

Targeted Covalent Inhibition of *Plasmodium* FK506 Binding Protein 35

Thomas C. Atack,* Donald D. Raymond, Christa A. Blomquist, Charisse Flerida Pasaje, Patrick R. McCarren, Jamie Moroco, Henock B. Befekadu, Foxy P. Robinson, Debjani Pal, Lisl Y. Esherick, Alessandra Ianari, Jacquin C. Niles, and William R. Sellers*

Cite This: *ACS Med. Chem. Lett.* 2020, 11, 2131−2138

Read Online

ACCESS | Metrics & More | Article Recommendations | Supporting Information

ABSTRACT: FK506-binding protein 35, FKBP35, has been implicated as an essential malarial enzyme. Rapamycin and FK506 exhibit antiplasmodium activity in cultured parasites. However, due to the highly conserved nature of the binding pockets of FKBPs and the immunosuppressive properties of these drugs, there is a need for compounds that selectively inhibit FKBP35 and lack the undesired side effects. In contrast to human FKBPs, FKBP35 contains a cysteine, C106, adjacent to the rapamycin binding pocket, providing an opportunity to develop targeted covalent inhibitors of *Plasmodium* FKBP35. Here, we synthesize inhibitors of FKBP35, show that they directly bind FKBP35 in a model cellular setting, selectively covalently modify C106, and exhibit antiplasmodium activity in blood-stage cultured parasites.

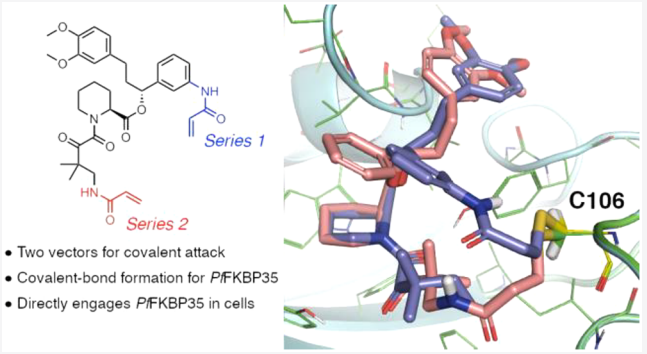

KEYWORDS: *FK506-binding protein, FKBP35, plasmodium, antimalarial, targeted covalent inhibition*

Malaria is caused by parasites of the genus *Plasmodium*. Worldwide, there are over 200 million cases every year. Despite progress in antimalarial therapies and in mosquito-control, over 400,000 people die annually, the majority resulting from *Plasmodium falciparum* (*Pf*).[1] Additionally, *Plasmodium vivax* (*Pv*) causes relapsing infection due to latent liver-stage parasites which remains a challenge for malaria eradication.[1,2] Finally, resistance to the frontline antimalarials is emerging, accelerating the need for new therapeutics with novel mechanisms of action.[3−5]

FK506-binding proteins (FKBP) are conserved throughout evolution and found across the *Plasmodium* genus.[6−8] Immunosuppression mediated by inhibitors of calcineurin and mTOR requires recruitment of FKBPs.[9−11] Specifically, FK506 and rapamycin (Figure 1) induce heterodimers between human FKBP12 and calcineurin or mTOR, respectively. As a result, FKBPs became targets in drug-discovery.[12,13]

In contrast to the 14 human FKPB isoforms, *Plasmodium* species have a single FKBP, FKBP35.[7,8] Interestingly, FK506 and rapamycin have antiplasmodium activity in blood-stage assays[6,14,15] and it has been hypothesized that inhibition of FKBP35 alone might suffice for antiparasitic activity.[6,14] Several groups have synthesized FKBP35-targeting compounds (Figure 1). Wandless et al. developed chimeric molecules consisting of the synthetic ligand for FKBP (**SLF**) conjugated

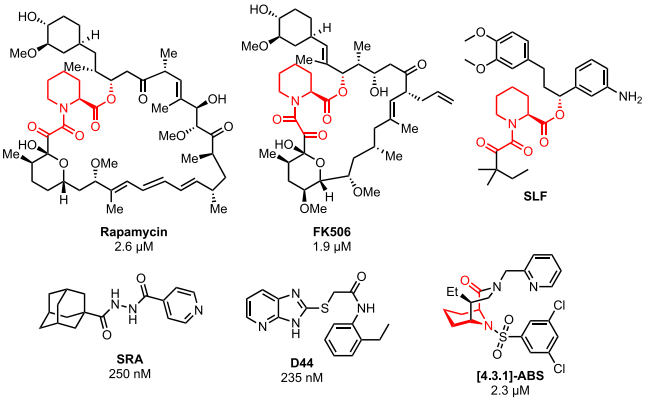

Figure 1. Structures of FKBP ligands with IC_{50}s in blood-stage antiplasmodium assays (SLF is untested against cultured parasites). The pipecolate binding motif common to the natural product ligands is in red.

Received: May 21, 2020
Accepted: September 1, 2020
Published: September 1, 2020

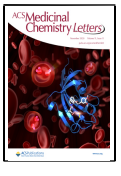

to methotrexate to deliver methotrexate to parasites through FKBP12 binding but did not report the antiplasmodium activity.[16] Compounds **SRA** and **D44** exhibited good antiplasmodium and PPIase activity despite lacking the pipecolate core common to many FKBP-binders (Figure 1, in red).[17,18] More recently, a library of novel [4.3.1]-aza-bicyclic sulfonamides ([**4.3.1**]-**ABS**) exhibited broad antimicrobial activity, including activity against *Plasmodium*.[19]

To date, all reported inhibitors show higher binding affinity for human FKBP12. This lack of selectivity is amplified by the cellular abundance of FKBP12 (4−5 μM in erythrocytes) versus FKBP35 (50−100 nM in *Plasmodium*).[16] A difficulty in achieving selectivity among different FKBPs is the highly conserved proline binding pocket where 13 out of 16 residues within 5 Å of rapamycin are identical between FKBP12 and *Pf*FKBP35. Interestingly, just outside of the binding pocket, *Pf*FKBP35 has a cysteine (C106) whereas FKBP12 has a histidine at this position. This cysteine is conserved across the human-infecting *Plasmodium* species and thus provides the opportunity to develop FKBP35 covalent inhibitors.[20] Such therapeutics might provide improved selectivity and prolonged duration of action and could be interesting for targeting the liver hypnozoite stage of *Plasmodium vivax*.

We began by modifying **D44** (Figure 1) to generate three analogues (Figure 2) and modeled binding of these analogues

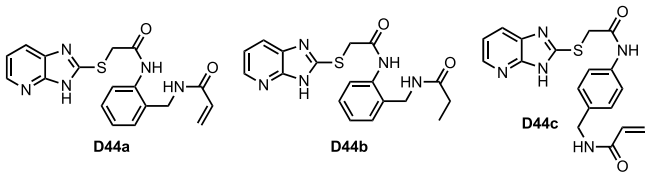

Figure 2. Structures of D44 derivatives from pilot study.

using the **D44**-FKBP35 structure (PDB 4J4N).[18,21] **D44a**, in which the terminal ethyl is substituted with a benzylic acrylamide, was predicted to occupy the same position as **D44** and bind favorably to C106. **D44b** replaces the acrylamide with a propionamide to serve as a noncovalent control, and in **D44c** the acrylamide is placed in an unfavorable position as a control for nonspecific cysteine-reactivity. By differential scanning calorimetry (DSC), none of these compounds showed a thermal shift against full-length FKBP12 or the *Pf*FKBP35 binding domain (FBD35) indicating absent binding compared to rapamycin. Additionally, we observed only trace, nonspecific covalent binding to C106 by mass spectrometry (Table S1). Together these data suggest that **D44** does not bind to FKBP35.

Next, we turned to **SLF** as a starting point.[16] As there are no structures of **SLF**-bound FKBP35 we used the structure of the related compound **SLFb** bound to human FKBP51(PDB 4DRK)[22] aligned with rapamycin-bound *Pf*FKBP35 (PDB 4QT2)[23] as the basis for docking. We noted two groups proximal to C106: the aryl ring of the benzylic ester (for Series 1) and the *tert*-pentyl group adjacent to the ketoamide (for Series 2, Figure 3a), and compounds from both series were modeled (Table S2). As a prototypical compound from Series 1, the model predicts covalently bound **1a** has good overlap with **SLFb** in the FKBP35 binding pocket (Figure 3b). Interestingly, covalently bound compounds from Series 2 show a greater degree of overlap with **SLFb** (Figure 3c) resulting in better docking scores than Series 1 compounds (Table S2).

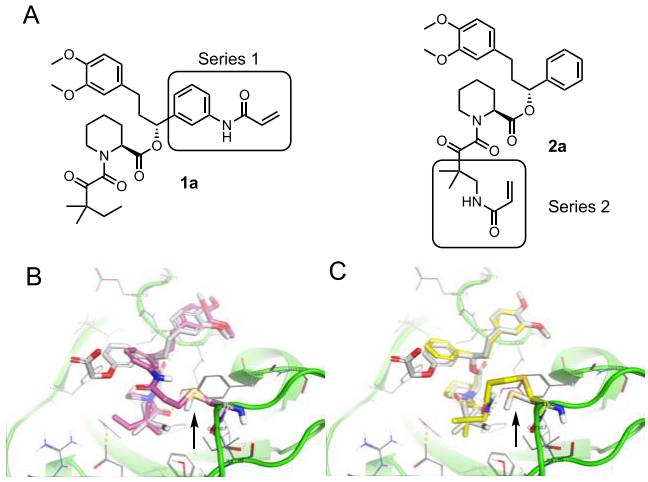

Figure 3. Docking studies of covalent **SLF** analogues. (A) Structures of representative compounds from Series 1 and Series 2. (B) Model structure of *1a* (purple) covalently bound to C106 (indicated by arrow) and docked in FBD35 with **SLFb** (gray) as a reference. (C) Model structure of *2a* (yellow) covalently bound to C106 (indicated by arrow) and docked in FBD35 with **SLFb** (gray) as a reference. Docking model based on alignment of **SLFb**-bound FKBP51 binding domain (PDB 4DRK) and rapamycin-bound FKBP35 binding domain (PDB 4QT2).

Next, we investigated both series to probe the reactivity of the cysteine and determine how the vector of the covalent bond between the ligand and FKBP35 influences compound binding.

For Series 1 (Scheme 1), a convergent synthesis was employed between pipecolic acid **3** or **4** with chiral benzylic alcohols **6a−d**. Compounds **5a−d** were synthesized via Claisen−Schmidt condensation between methylvanillin and 2′-, 3′-, or 4′-nitroacetophenone followed by hydrogenation. *meta*-Aniline **5b** was Boc-protected to generate compound **6b**. Coupling of **3** and **6b** followed by Boc-deprotection furnished **SLF**, which was acylated with acryloyl chloride to produce **1a** or propionyl chloride to produce **1b**. Compounds **1c** and **1d** required an alternate synthetic pathway since the free anilines resulted in rapid decomposition. In order to avoid this decomposition pathway, intermediates **5a** and **5c** were acylated with 3-chloropropionyl chloride and then coupled with **3**. Elimination of the β-chlorine with NEt_3 generated compounds **1c** and **1d**. **SLFb** was synthesized by coupling benzylic alcohol **6d** with **3** followed by deprotection of the acid. Compounds **1e** and **1f** were synthesized similarly to **1a** and **1c** using **4** as the coupling partner with **5b** and **5a**, respectively.

We investigated the binding of these compounds in two orthogonal assays: DSC and fluorescence polarization (FP, Table 1). All compounds were screened against recombinant FBD35 and FKBP12 to investigate selectivity.

Previous studies have shown that **SLF** has >10-fold lower affinity for FKBP35 than FKBP12;[16] however, we observe a less profound difference in affinities. The addition of the covalent warhead to this compound (**1a**) does not drastically alter the IC_{50} as measured by FP. However, we observe a large thermal shift of +13.4 °C by DSC. Saturation of the acrylamide to the propionamide (**1b**) improves the binding by FP slightly but reduces the thermal shift to +2.9 °C, suggesting that the ability to form a covalent bond makes for a more thermodynamically stable complex. Moving the acrylamide warhead to the *ortho* position (**1c**) showed >10-fold weaker

https://dx.doi.org/10.1021/acsmedchemlett.0c00272
ACS Med. Chem. Lett. 2020, 11, 2131−2138

Scheme 1. Synthesis of Series 1 Compounds[a]

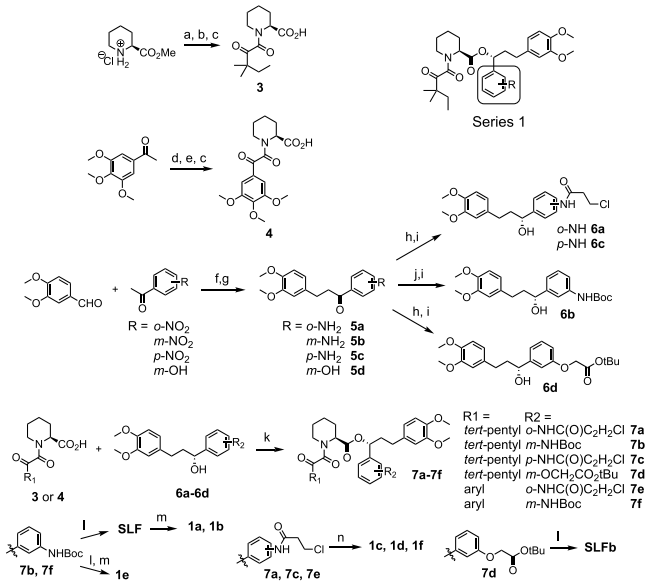

[a]Reagents and conditions: (a) Methyl oxalyl chloride, DIPEA, DCM, 22 °C, 6 h; (b) 1,1-dimethylpropylmagnesium chloride, THF, −78 °C, 2 h; (c) LiOH, MeOH, 0−25 °C, 12 h; (d) SeO_2, pyridine, 110 °C, 3 h; (e) oxalyl chloride, DMF, DCM, 0 °C, 30 m *then:* pipecolic acid methyl ester, NEt_3, DCM, 0 °C, 2 h; (f) KOH, EtOH, 0 °C, 12 h; (g) H_2, Pd/C, EtOAc, 2−24 h; (h) 3-chloropropionoyl chloride OR *tert*-butyl bromoacetate, K_2CO_3, acetone, 22 °C, 16 h; (i) (+)-DIP-chloride, THF, −45 °C, 16 h *then:* diethanolamine, Et_2O, 22 °C, 2 h; (j) Boc_2O, 1,4-dioxane, 150 °C, 4 h; (k) DCC, DMAP, DCM, 22 °C, 2 h; (l) TFA, DCM, 22 °C, 2 h; (m) acryloyl chloride OR propionyl chloride, NEt_3, DCM, 0 °C, 2 h; (n) NEt_3, MeCN, 80 °C, 6−18 h.

Table 1. Binding of Series 1 Ligands to FBD35 and FKBP12

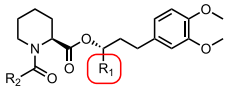

	R1	R2	FBD35 IC_{50}[a]	FBD35 ΔT_M[b]	FKBP12 IC_{50}	FKBP12 ΔT_M
1a	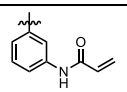		206*	13.4	132	5.6
1b	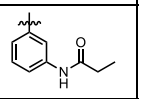		76	2.8	58	6.8
1c	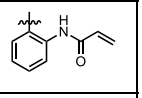		2,851*	9.6	423	3.2
1d	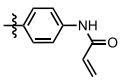		85	2.3	100	6
SLF	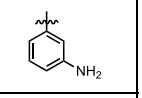		177*	2.9	70	0.4
SLFb	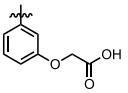		761	2.8	27	6.6
1e	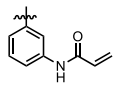	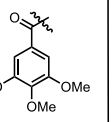	NB	1.5	326	4.9
1f	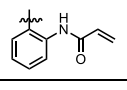		NB	-1.3	3,268	1.4

[a]Determined by fluorescence polarization and fitting the data to a competitive inhibition model (nM). [b]Determined by differential scanning calorimetry (°C). *Incomplete displacement of fluorescent probe.

binding by FP but retained a large thermal shift of +9.6 °C. To rule out the possibility of nonspecific covalent bond formation, compound **1d** was synthesized where the acrylamide is predicted to angle away from C106. **1d** maintains good binding by FP and a thermal shift close to other noncovalent controls, suggesting that the large thermal shifts we observe result from covalent bond formation.

Concerned about the lipophilicity and solubility of these compounds (**1a** cLogP = 5.0, PBS pH 7.4 solubility = 0.31 μM; **1c** cLogP = 4.4, PBS pH 7.4 solubility = 3.5 μM), we investigated swapping the *tert*-pentyl moiety for a 3,4,5-trimethoxybenzyl as ligands with this modification retain good affinity for human FKBPs.[24] As predicted, this change resulted in a decrease in the cLogP (3.6 for **1e** and 3.0 for **1f**) and a concomitant increase in PBS solubility (3.1 μM and 23 μM, respectively). However, no binding to FBD35 was detected by FP, and only **1e** displayed weak binding by DSC. Compound **1f** resulted in a negative DSC shift indicating a destabilizing interaction with FBD35. Both **1e** and **1f** were able to bind to FKBP12 albeit with lower affinity when compared to **1a** or **1c.** These data indicate that despite the high homology between the binding pockets, FKBP35 cannot accommodate large aryl rings.

For Series 2, we examined both alkyl (**2a**−**2e**, **2h**) and aryl (**2f**, **2g**) acrylamides and acrylates. The synthesis of Series 2 required a change in strategy compared to Series 1 (Scheme 2). Compounds **2c**−**2g** were synthesized from common intermediate **8a**, which was generated from the coupling of **6e** with Boc-protected pipecolic acid. **2h** was similarly synthesized from intermediate **8b**. Following the strategy of Holt et al.,[25] 4,4-dimethyldihydrofuran-2,3-dione was heated with **8a** or **8b** in the presence of DMAP to form intermediates **9a** and **9b**. Acylation of the resultant alcohol with acryloyl chloride or propionyl chloride generated esters **2c**, **2d**, and **2h**. Inspired by this strategy, aryl acrylamides **2f** and **2g** were synthesized by the reaction between **8a** and a Boc-protected isatin derivative followed by Boc-deprotection and acylation of the resultant aniline. Attempts to convert the alcohol of **9a** into an amine in order to access **2a** and **2b** were unsuccessful. In order to place an acrylamide in this position, **8a** was coupled with Boc-protected *gamma*-aminobutyric acid to synthesize **2e**, which lacks the ketone and geminal dimethyl groups that were previously shown to enhance FKBP-binding affinity.[26]

Recognizing that the precursor to **2a** and **2b** was a *beta*-amino carbonyl, we envisioned that a Mannich reaction could provide access to these compounds. To test this, intermediate **11** was generated by *tert*-butyl protection of Cbz-protected pipecolic acid, Cbz-deprotection, and subsequent coupling with 3-methyl-2-oxobutanoic acid. **11** was treated with *para*-methoxybenzylamine and aqueous formaldehyde to form the Mannich adduct, which was acylated with either 3-chloropropionoyl chloride or propionyl chloride to generate **12a** and **12b**. Oxidative deprotection of the benzylic amide followed by TFA treatment gave intermediates **13a** and **13b**

https://dx.doi.org/10.1021/acsmedchemlett.0c00272
ACS Med. Chem. Lett. 2020, 11, 2131−2138

Scheme 2. Synthesis of Series 2 Compounds[a]

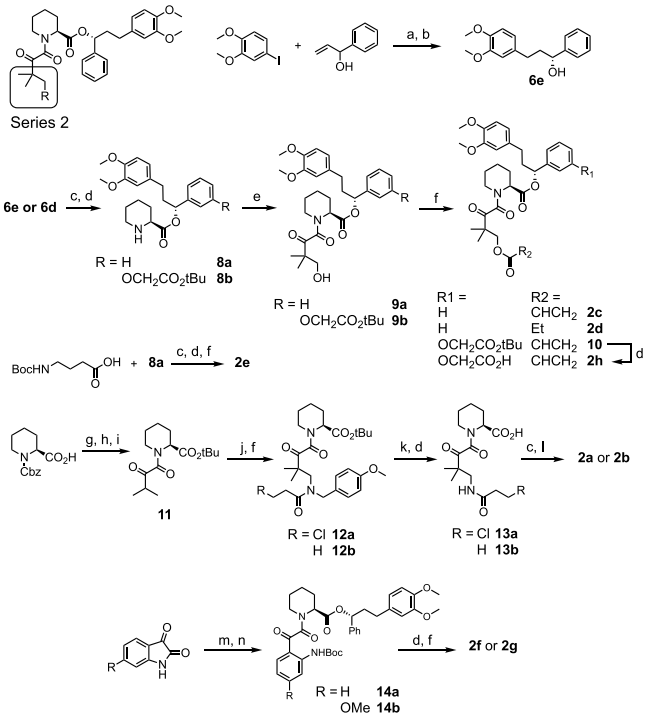

[a]Reagents and conditions: (a) $Pd(OAc)_2$, NEt_3, DMF, 80 °C, 16 h; (b) (+)-DIP-chloride, THF, −45 °C, 6 h *then:* diethanolamine, Et_2O, 22 °C, 2 h; (c) DCC, Boc-Pip-OH, DMAP, DCM, 0 °C, 2 h; (d) TFA, DCM, 22 °C, 2 h; (e) 4,4-dimethyldihydrofuran-2,3-dione, DMAP, toluene, 80 °C, 16 h; (f) acryloyl chloride OR propionyl chloride, NEt_3, DCM, 0 °C, 2−18 h; (g) DCC, tBuOH, DMAP, DCM, 0 °C, 2 h; (h) H_2, Pd/C, EtOH, 1 h; (i) DCC, 3-methyl-2-oxobutanoic acid, DMAP, DCM, 0 °C, 2 h; (j) formaldehyde, *para*-methoxybenzylamine, MeOH, H_2O, 50 °C, 44 h; (k) CAN, MeCN/H_2O, 16 h; (l) EDC, DMAP, DCM, 0 °C, 12 h; (m) Boc_2O, DMAP, THF, 6 h; (n) **8a**, DMAP, toluene, 80 °C, 2 h.

Table 2. Binding of Series 2 Ligands to FBD35 and FKBP12

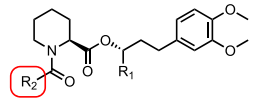

	R1	R2	FBD35 IC_{50}[a]	FBD35 ΔT_M[b]	FKBP12 IC_{50}	FKBP12 ΔT_M
2a		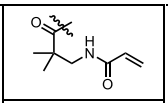	104	15.2	23	8.8
2b		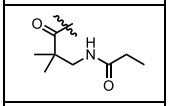	92	4.3	40	7.7
2c		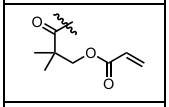	559	14.5	166	5.2
2d		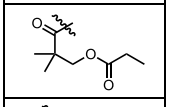	99	3	43	5.9
2e		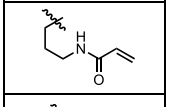	2,641	13.8	3,247	7.9
2f		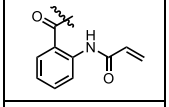	NB	0.4	NB	0.2
2g		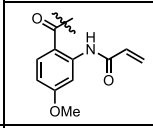	NB	0.0	NB	0.1
2h	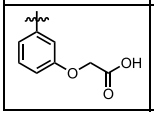	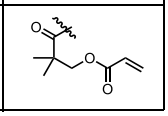	137	16.3	38	6.2

[a]Determined by fluorescence polarization and fitting the data to a competitive inhibition model (nM). [b]Determined by differential scanning calorimetry (°C).

which were then coupled with **6e** to complete the syntheses of **2a** and **2b**.

In our covalent docking model, **2a** and **2c** were predicted to form more stable covalent complexes than **1a** or **1c** (Table S2). While the IC_{50}s overall did not change significantly between the two series, we observed larger thermal shifts in the DSC. As observed in Series 1, this large shift was dramatically reduced upon removal of the Michael acceptor (**2b** and **2d**) indicating that Series 2 compounds can likely form a covalent bond with FBD35. Removal of the ketone and geminal dimethyl from **2a** (**2e**) significantly lowered binding affinity but maintained the large thermal shift. Despite the predictions of robust binding with **2f** or **2g** in the docking model (Table 2), we saw no binding in the FP or DSC assays for either protein providing additional evidence that FKBP35 cannot accommodate aryl rings within the binding pocket. Similar to the solubility issues in Series 1, several of the Series 2 compounds have poor solubility and high cLogP values. In particular, **2c** has a cLogP of 4.4 and a PBS solubility of <0.1 μM. By contrast, **SLFb** has a similar cLogP of 4.1 but a PBS solubility of 59 μM. Adding this free carboxylate to **2c** to generate **2h** reduced the cLogP to 3.5 while PBS solubility improved to 70 μM. Further, this compound exhibited a very good IC_{50} and the largest thermal shift recorded.

We predict that this large shift in T_m is a result of a covalent bond between these ligands and C106. In support of this, all of the covalent compounds that were able to bind to FBD35 by FP also exhibited much larger thermal shifts (>9 °C vs 2−4 °C, generally) relative to their noncovalent controls (**1a** vs **1b**, **2a** vs **2b**, **2c** vs **2d**, and **1c**, **2e**, and **2h**). Notably, we observed two distinct melting points in the DSC traces for putative covalent compounds that were recorded after short incubations with FBD35. To highlight this phenomenon, compound **1c** was measured by DSC after a short incubation time with FBD35 and FKBP12. When incubated with FBD35, we observe two overlapping melting curves with distinct ΔT_m at 1.6 and 9.6 °C relative to the apoprotein (Figure 4a). Repeating the same experiment with FKBP12 results in a single ΔT_m of 3.2 °C (Figure 4b). The first ΔT_m is likely indicative of the overall weaker affinity of **1c** for FBD35, which is corroborated by our FP results. This ΔT_m is within the same range of all the noncovalent controls, which we interpret as resulting from a reversible ligand−protein interaction. With extended incubation times (>24 h), we observe only the second, larger thermal shift with the covalent compounds whereas the noncovalent controls remain unchanged (data not shown). All compounds showed only a single thermal shift when tested against human FKBP12, regardless of incubation time.

https://dx.doi.org/10.1021/acsmedchemlett.0c00272
ACS Med. Chem. Lett. 2020, 11, 2131−2138

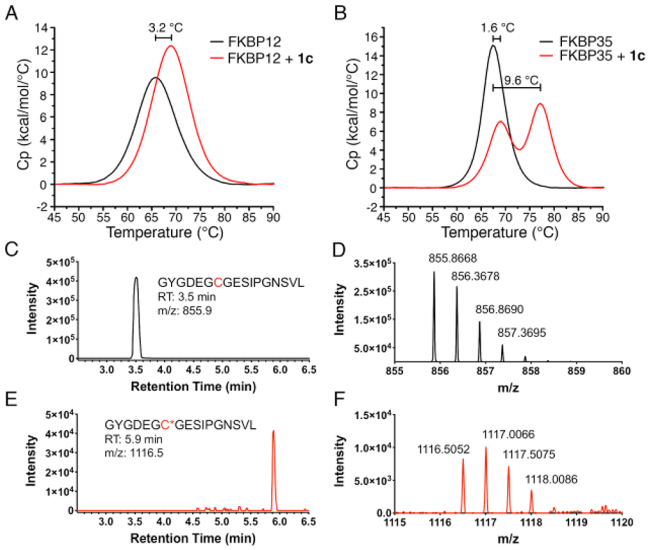

Figure 4. Evidence for covalent bond formation between **1c** and FBD35 observed in DSC and confirmed by LC-MS. (A) DSC trace of **1c** measured on FBD showing two distinct melting curves at Δ = 1.6 °C and Δ = 9.6 °C. (B) DSC trace of **1c** on FKBP12 showing a single melting curve shift at Δ = 3.2 °C. (C) Extracted ion chromatogram of iodoacetamide-treated, chymotrypsin-digested FBD35 found the expected carbamidomethylated peptide (GYGDEGCGESIPGN, m/z = 855.9, 2nd charge state) at RT = 3.5 min. (D) Mass spectrum of the peak at 3.5 min in panel C. (E) Extracted ion chromatogram of **1c**-treated, chymotrypsin-digested FBD35 found the expected **1c**-modified peptide (GYGDEGC*GESIPGN, m/z = 1116.5, 2nd charge state) at RT = 5.9 min. (F) Mass spectrum of the peak at 5.9 min in panel E.

To confirm the formation of a covalent adduct, we analyzed FBD35 by LC-MS alone or after 24 h of incubation with **1c** (Figure S1). After extended incubation with **1c**, we observed a nearly 1 min shift in the retention time of the protein complex vs the apo protein with an increase of mass to 14.5 kDa, consistent with the expected mass of the apo protein (13.9 kDa) plus the ligand (579 Da). Additionally, we subjected both the FBD35 apoprotein and the **1c**-FBD35 adduct to enzymatic digestion to generate the peptide containing C106 (GYGDEGCGESIPGN, Figure 4c–f, Figure S1). In the extracted ion chromatogram of the apoprotein, the carbamidomethylated peptide was found at 3.5 min (Figure 4c) with the correct mass (m/z = 855.9, second charge state, Figure 4d). When incubated with **1c**, there was some residual unmodified peptide found at 3.5 min (Figure S1c–d) as well as the predicted **1c**-inclusion peptide at RT = 5.9 (Figure 4e) with the correct mass (m/z = 1116.5, second charge state, Figure 4f). This mass was not found in the untreated protein (Figure S1e–f).

We next determined the relative rates of covalent adduct formation and FKBP35 consumption (Figure S2a,b) for compounds **1a–c**, **2a**, and **2c** via LC-MS. Measuring the reaction half-life reveals a rank order of **2c** > **1c** > **2a** > **1a** and no binding by **1b** (Figure S2c). Given their highly conserved structures, the stark difference in reaction half-lives between **2c** ($t_{1/2}$ = 0.78 h) and **2a** ($t_{1/2}$ = 11.7 h) is likely a result of the difference in reactivities between acrylates and acrylamides,[27] highlighting the importance of fine-tuning warhead electrophilicity.

We next were interested in comparing the interaction of compounds with FKBP35 and human FKBP12 in a consistent cellular setting. To this end we employed a nanoluciferase bioluminescent resonant energy transfer (nanoBRET) assay to measure target engagement.[28] We generated HEK293T cells stably expressing either nanoluciferase-tagged (nLuc) full length *Pf*FKBP35 or nLuc-tagged FKBP12 (Figure S3). Using a BODIPY-conjugated rapamycin tracer (**Rap-Gly-BDP**), we were able to measure the interaction with both FKBPs and measure its displacement in cells with unlabeled compounds to infer direct target engagement (Figure S4).

As a positive control we measured displacement of the tracer with unmodified rapamycin (Figure 5a,b black squares) and

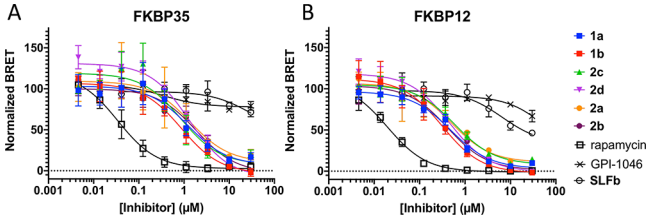

Figure 5. Intracellular binding of compounds to FKBP35 and FKBP12 in a NanoBRET cellular target engagement assay. (A) Normalized BRET ratio of covalent and noncovalent matched pairs in HEK-293T cells expressing nLuc-tagged FKBP35. (B) Normalized BRET ratio of covalent and noncovalent matched pairs in HEK-293T cells expressing nLuc-tagged FKBP12.

found robust tracer displacement with IC_{50}s of 34 nM (FKBP35) and 20 nM (FKBP12), respectively (Table S3). As a negative control, we measured tracer displacement using GPI-1046 (Figure S5), an early FKBP12 ligand[29] of similar structure to SLF whose ability to bind FKBPs was subsequently called into question.[22,30] We proceeded to measure matched pairs **1a** and **1b**, **2a** and **2b**, and **2c** and **2d** in the assay. After a 2 h incubation all compounds displace the fluorescent tracer, providing evidence that these compounds not only engage with FKBPs but are also cell permeable. Despite submicromolar IC_{50} values against both FKBPs in the FP assay **SLFb** displayed markedly reduced probe displacement likely due to reduced cell permeability as a result of the free carboxylate. Similar to the FP assay, there were no significant differences between covalent and noncovalent compounds in this assay. This suggests the intrinsic binding of the compounds remains a major driver of target affinity at 2 h. Nonetheless, the NanoBRET assay confirms that these compounds are not only cell-permeable but can also directly engage the target FKBP in a cellular setting.

Given the success of our biochemical assays, we investigated the activity of compounds **1a** and **1b** on live, cultured parasites (Figure 6). Using a luciferase reporter NF54 *P. falciparum* parasite line, both **1a** (IC_{50} = 1.4 μM) and **1b** (IC_{50} = 1.9 μM) showed dose-dependent growth-inhibition (Figure 6a). Gratifyingly, these compounds performed similarly to unmodified rapamycin (IC_{50} = 1.1 μM). Despite displaying poorer binding in the FP assay, **1c** shows similar antiplasmodium activity as **1a** (IC_{50} = 1.9 μM), possibly linked to faster adduct formation with FKBP35 (Figure S2c). As we observed in the NanoBRET assay, **SLFb** (IC_{50} = 33.7 μM) performs poorly compared to **1a** and **1b** (Figure 6b). Despite similar affinity and higher warhead reactivity, **2c** also performs poorly in this assay (IC_{50} = 13 μM, Figure S6a). This discrepancy is likely due to differences in plasma stability as **2c** is rapidly degraded by plasma where **1a–c** are not (Figure S6b). Additionally, these compounds were not cytotoxic in HEK293T cells across the relevant

https://dx.doi.org/10.1021/acsmedchemlett.0c00272
ACS Med. Chem. Lett. 2020, 11, 2131–2138

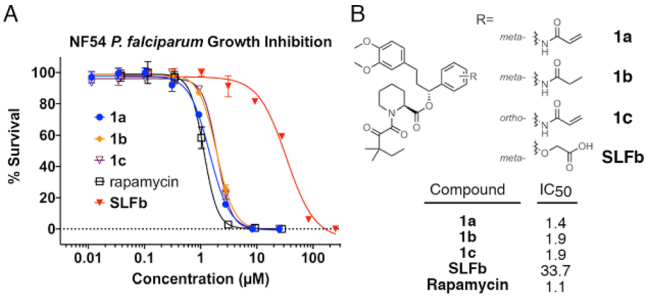

Figure 6. *P. falciparum* strain NF54 growth-inhibition assay. (A) NF54 parasites were incubated with **1a**, **1b**, **SLFb**, or rapamycin in a dose-dependent manner. Proliferation was measured by luminescence after a complete life-cycle and normalized to DMSO (100%) and chloroquine (100 nM, 0%). (B) Structural differences between synthetic ligands and compound IC_{50}s (μM).

concentration range indicating that the *Plasmodium* assay data are not a result of general cytotoxicity (Figure S7).

While the *in vitro* data confirm these compounds covalently modify C106 and the NanoBRET assay demonstrates direct target engagement of FKBP35 in a cellular context, additional genetic studies will be necessary to fully establish whether FKBP35 inhibition is responsible for their antiplasmodium activity. Despite this limitation, our results suggest that covalent inhibition of FKBP35 could be an avenue for the development of antimalarial therapeutics. The presence of C106 provides a functional handle for high-throughput screening of covalent fragment libraries for the development of novel chemical matter that could provide improved selectivity between FKBP35 and the human FKBPs. While we predominantly examined simple acrylamides, the slow rate of covalent-bond formation indicates more electrophilic warheads might prove beneficial for additional selectivity and potency. In fact, switching to a more reactive acrylate drastically accelerated the rate of covalent bond formation but at the cost of plasma stability. Additional experiments examining warhead reactivity should be a fruitful endeavor. Alternatively, it is possible that the pipecolic acid core does not provide an optimal foundation upon which to covalently attack C106. Thus, screening efforts to uncover new high affinity FKBP-binding chemotypes optimized for the covalent modification strategy presented here have the potential to create more potent and selective compounds for this highly conserved enzyme. Such compounds will be of significant interest for testing against liver-stage disease.

■ ASSOCIATED CONTENT

Supporting Information

The Supporting Information is available free of charge at https://pubs.acs.org/doi/10.1021/acsmedchemlett.0c00272.

Synthesis and characterization of all compounds and biophysical, biochemical, and biological assay procedures (PDF)

■ AUTHOR INFORMATION

Corresponding Authors

Thomas C. Atack − *Broad Institute of MIT and Harvard, Cambridge, Massachusetts 02142, United States;* orcid.org/0000-0001-5953-2261; Email: tatack@broadinstitute.org

William R. Sellers − *Broad Institute of MIT and Harvard, Cambridge, Massachusetts 02142, United States; Dana-Farber Cancer Institute, Boston, Massachusetts 02215, United States; Harvard Medical School, Boston, Massachusetts 02115, United States;* Email: wsellers@broadinstitute.org

Authors

Donald D. Raymond − *Broad Institute of MIT and Harvard, Cambridge, Massachusetts 02142, United States*

Christa A. Blomquist − *Broad Institute of MIT and Harvard, Cambridge, Massachusetts 02142, United States*

Charisse Flerida Pasaje − *Department of Biological Engineering, Massachusetts Institute of Technology, Cambridge, Massachusetts 02139, United States*

Patrick R. McCarren − *Broad Institute of MIT and Harvard, Cambridge, Massachusetts 02142, United States*

Jamie Moroco − *Broad Institute of MIT and Harvard, Cambridge, Massachusetts 02142, United States;* orcid.org/0000-0001-8250-5923

Henock B. Befekadu − *Broad Institute of MIT and Harvard, Cambridge, Massachusetts 02142, United States*

Foxy P. Robinson − *Broad Institute of MIT and Harvard, Cambridge, Massachusetts 02142, United States*

Debjani Pal − *Broad Institute of MIT and Harvard, Cambridge, Massachusetts 02142, United States*

Lisl Y. Esherick − *Department of Biological Engineering, Massachusetts Institute of Technology, Cambridge, Massachusetts 02139, United States*

Alessandra Ianari − *Broad Institute of MIT and Harvard, Cambridge, Massachusetts 02142, United States*

Jacquin C. Niles − *Department of Biological Engineering, Massachusetts Institute of Technology, Cambridge, Massachusetts 02139, United States;* orcid.org/0000-0002-6250-8796

Complete contact information is available at: https://pubs.acs.org/10.1021/acsmedchemlett.0c00272

Author Contributions

T.C.A., A.I., and W.R.S. generated the concept and experiments. T.C.A. designed and synthesized all compounds, analyzed data, and prepared the manuscript. D.D.R. prepared and isolated recombinant proteins and ran DSC experiments and mass spec assays. C.A.B. performed cell culture and nanoBRET experiments. C.F.P. and L.Y.E. performed and analyzed parasite viability experiments. P.R.M. performed computational modeling. T.C.A. and H.B.B. performed FP experiments. J.M. ran and with T.C.A. analyzed mass spec experiments. F.P.R. and D.P. performed cell viability experiments. A.I. and J.C.N. facilitated the collaboration. All authors discussed the results and commented on the manuscript. All authors have given approval to the final version of the manuscript.

Funding

This research was supported by The Broad Institute (SPARC grant (T.C.A., D.D.R., W.R.S.) and Broad Next10 (J.C.N)) and The Bill and Melinda Gates Foundation (OPP1158199 and OPP1162467 (C.F.A.P., L.Y.E., J.C.N.)).

Notes

The authors declare the following competing financial interest(s): W.R.S. is a Board or SAB member and holds equity in Peloton Therapeutics, Ideaya Biosciences, Civetta Therapeutics, and Bluebird and has consulted for Array, Astex, Dynamo Therapeutics, Ipsen, PearlRiver Therapeutics, Sanofi,

https://dx.doi.org/10.1021/acsmedchemlett.0c00272
ACS Med. Chem. Lett. 2020, 11, 2131−2138

and Servier and receives research funding from Pfizer Pharmaceuticals and Deerfield Management.

Biographies

Thomas Atack received his Ph.D. degree from Indiana University Bloomington where he developed novel iron- and manganese-catalyzed cross-coupling reactions under Prof. Silas Cook. He then transitioned to the Broad Institute of MIT and Harvard where he joined the research group of Dr. William R. Sellers to study therapeutic development for diseases with unmet medical need. His research interests revolve around the design, synthesis, and characterization of novel chemical matter for therapeutic development.

William Sellers is a physician-scientist, Core Institute Member at the Broad Institute and a Professor of Medicine at the Dana-Farber Cancer Institute and Harvard Medical School. He directs a research group focused on utilizing functional genomic technologies to discover new targets and new therapeutics in cancer. He is a co-founder of Civetta Therapeutics. Previously, Dr. Sellers directed cancer drug discovery and early cancer clinical development at the Novartis, led the Cancer Cell Line Encyclopedia project, co-discovered EGFR mutations in lung cancer and served on the National Cancer Advisory Board.

■ ACKNOWLEDGMENTS

The authors thank Eamon Comer for thoughtful chemistry discussions; Dale Porter for helping secure internal funding sources; and Christian Stephan Meyners and Wei Jiang for assistance with the fluorescence polarization assay.

■ ABBREVIATIONS

FKBP, FK506 binding protein; FBD, FKBP binding domain; SLF, synthetic ligand for FKBP; PPIase, peptidyl prolyl isomerase; DSC, differential scanning calorimetry; FP, fluorescence polarization; nLuc, nanoluciferase; BRET, bioluminescent resonant energy transfer

■ REFERENCES

(1) WHO. *World Malaria Report 2017*; 2017.
(2) Baird, J. K. Real-World Therapies and the Problem of Vivax Malaria. *N. Engl. J. Med.* **2008**, *359* (24), 2601−2603.
(3) Corey, V. C.; Lukens, A. K.; Istvan, E. S.; Lee, M. C. S.; Franco, V.; Magistrado, P.; Coburn-Flynn, O.; Sakata-Kato, T.; Fuchs, O.; Gnädig, N. F.; Goldgof, G.; Linares, M.; Gomez-Lorenzo, M. G.; De Cózar, C.; Lafuente-Monasterio, M. J.; Prats, S.; Meister, S.; Tanaseichuk, O.; Wree, M.; Zhou, Y.; Willis, P. A.; Gamo, F.-J.; Goldberg, D. E.; Fidock, D. A.; Wirth, D. F.; Winzeler, E. A. A Broad Analysis of Resistance Development in the Malaria Parasite. *Nat. Commun.* **2016**, *7* (May), 11901.
(4) Trape, J. F.; Pison, G.; Preziosi, M. P.; Enel, C.; Du Loû, A. D.; Delaunay, V.; Samb, B.; Lagarde, E.; Molez, J. F.; Simondon, F. Impact of Chloroquine Resistance on Malaria Mortality. *C. R. Acad. Sci., Ser. III* **1998**, *321* (8), 689−697.
(5) Das, D.; Phyo, A. P.; Tarning, J.; Ph, D.; Lwin, K. M.; Ariey, F.; Hanpithakpong, W.; Lee, S. J.; Ringwald, P.; Silamut, K.; Herdman, T.; An, S. S.; Yeung, S.; Socheat, D.; White, N. J. Artemisinin Resistance in Plasmodium Falciparum Malaria. *N. Engl. J. Med.* **2009**, *361* (5), 455−467.
(6) Monaghan, P.; Fardis, M.; Revill, W. P.; Bell, A. Antimalarial Effects of Macrolactones Related to FK520 (Ascomycin) Are Independent of the Immunosuppressive Properties of the Compounds. *J. Infect. Dis.* **2005**, *191* (July), 1342−1349.
(7) Monaghan, P.; Bell, A. A Plasmodium Falciparum FK506-Binding Protein (FKBP) with Peptidyl-Prolyl Cis-Trans Isomerase and Chaperone Activities. *Mol. Biochem. Parasitol.* **2005**, *139* (2), 185−195.
(8) Bell, A.; Monaghan, P.; Page, A. P. Peptidyl-Prolyl Cis−Trans Isomerases (Immunophilins) and Their Roles in Parasite Biochemistry, Host−Parasite Interaction and Antiparasitic Drug Action. *Int. J. Parasitol.* **2006**, *36* (3), 261−276.
(9) Van Duyne, G.; Standaert, R.; Karplus, P.; Schreiber, S.; Clardy, J. Atomic Structure of FKBP-FK506, an Immunophilin-Immunosuppressant Complex. *Science (Washington, DC, U. S.)* **1991**, *252* (5007), 839−842.
(10) Michnick, S. W.; Rosen, M. K.; Wandless, T. J.; Karplus, M.; Schreiber, S. L. Solution Structure of FKBP, a Rotamase Enzyme and Receptor for FK506 and Rapamycin. *Science (Washington, DC, U. S.)* **1991**, *252* (5007), 836−839.
(11) Banaszynski, L. A.; Liu, C. W.; Wandless, T. J. Characterization of the FKBP-Rapamycin-FRB Ternary Complex. *J. Am. Chem. Soc.* **2005**, *127* (13), 4715−4721.
(12) Kolos, J. M.; Voll, A. M.; Bauder, M.; Hausch, F. FKBP Ligands—Where We Are and Where to Go? *Front. Pharmacol.* **2018**, *9* (December), DOI: 10.3389/fphar.2018.01425
(13) Dunyak, B. M.; Gestwicki, J. E. Peptidyl-Proline Isomerases (PPIases): Targets for Natural Products and Natural Product-Inspired Compounds. *J. Med. Chem.* **2016**, *59* (21), 9622−9644.
(14) Monaghan, P.; Leneghan, D. B.; Shaw, W.; Bell, A. The Antimalarial Action of FK506 and Rapamycin: Evidence for a Direct Effect on FK506-Binding Protein PfFKBP35. *Parasitology* **2017**, *144* (7), 869−876.
(15) Nsanzabana, C.; Rosenthal, P. J. In Vitro Activity of Antiretroviral Drugs against Plasmodium Falciparum. *Antimicrob. Agents Chemother.* **2011**, *55* (11), 5073−5077.
(16) Braun, P. D.; Barglow, K. T.; Lin, Y. M.; Akompong, T.; Briesewitz, R.; Ray, G. T.; Haldar, K.; Wandless, T. J. A Bifunctional Molecule That Displays Context-Dependent Cellular Activity. *J. Am. Chem. Soc.* **2003**, *125* (25), 7575−7580.
(17) Harikishore, A.; Leow, M. L.; Niang, M.; Rajan, S.; Pasunooti, K. K.; Preiser, P. R.; Liu, X.; Yoon, H. S. Adamantyl Derivative as a Potent Inhibitor of Plasmodium FK506 Binding Protein 35. *ACS Med. Chem. Lett.* **2013**, *4* (11), 1097−1101.
(18) Harikishore, A.; Niang, M.; Rajan, S.; Preiser, P. R.; Yoon, H. S. Small Molecule Plasmodium FKBP35 Inhibitor as a Potential Antimalaria Agent. *Sci. Rep.* **2013**, *3*, 2501.
(19) Pomplun, S.; Sippel, C.; Hähle, A.; Tay, D.; Shima, K.; Klages, A.; Ünal, C. M.; Rieß, B.; Toh, H. T.; Hansen, G.; Yoon, H. S.; Bracher, A.; Preiser, P.; Rupp, J.; Steinert, M.; Hausch, F. Chemogenomic Profiling of Human and Microbial FK506-Binding Proteins. *J. Med. Chem.* **2018**, *61* (8), 3660−3673.
(20) MacDonald, C. A.; Boyd, R. J. Molecular Docking Study of Macrocycles as Fk506-Binding Protein Inhibitors. *J. Mol. Graphics Modell.* **2015**, *59*, 117−122.
(21) Zhu, K.; Borrelli, K. W.; Greenwood, J. R.; Day, T.; Abel, R.; Farid, R. S.; Harder, E. Docking Covalent Inhibitors: A Parameter Free Approach to Pose Prediction and Scoring. *J. Chem. Inf. Model.* **2014**, *54* (7), 1932−1940.
(22) Gopalakrishnan, R.; Kozany, C.; Gaali, S.; Kress, C.; Hoogeland, B.; Bracher, A.; Hausch, F. Evaluation of Synthetic FK506 Analogues as Ligands for the FK506-Binding Proteins 51 and 52. *J. Med. Chem.* **2012**, *55* (9), 4114−4122.
(23) Bianchin, A.; Allemand, F.; Bell, A.; Chubb, A. J.; Guichou, J. F. Two Crystal Structures of the FK506-Binding Domain of Plasmodium Falciparum FKBP35 in Complex with Rapamycin at High Resolution. *Acta Crystallogr., Sect. D: Biol. Crystallogr.* **2015**, *71*, 1319−1327.
(24) Armistead, D. M.; Badia, M. C.; Deininger, D. D.; Duffy, J. P.; Saunders, J. O.; Tung, R. D.; Thomson, J. A.; DeCenzo, M. T.; Futer, O.; Livingston, D. J.; Murcko, M. A.; Yamashita, M. M.; Navia, M. A. Design, Synthesis and Structure of Non-Macrocyclic Inhibitors of FKBP12, the Major Binding Protein for the Immunosuppressant FK506. *Acta Crystallogr., Sect. D: Biol. Crystallogr.* **1995**, *51* (4), 522−528.
(25) Holt, D. A.; Luengo, J. I.; Yamashita, D. S.; Oh, H. J.; Konialian, A. L.; Yen, H. K.; Rozamus, L. W.; Brandt, M.; Bossard, M. J.; Levy, M. A.; Eggleston, D. S.; Liang, J.; Schultz, L. W.; Stout, T. J.; Clardy, J.

https://dx.doi.org/10.1021/acsmedchemlett.0c00272
ACS Med. Chem. Lett. 2020, 11, 2131−2138

Design, Synthesis, and Kinetic Evaluation of High-Affinity FKBP Ligands and the X-Ray Crystal Structures of Their Complexes with FKBP12. *J. Am. Chem. Soc.* **1993**, *115* (22), 9925−9938.
(26) Holt, D. A.; Konialian-Beck, A. L.; Oh, H. J.; Yen, H. K.; Rozamus, L. W.; Krog, A. J.; Erhard, K. F.; Ortiz, E.; Levy, M. A.; Brandt, M.; Bossard, M. J.; Luengo, J. I. Structure-Activity Studies of Synthetic FKBP Ligands as Peptidyl-Prolyl Isomerase Inhibitors. *Bioorg. Med. Chem. Lett.* **1994**, *4* (2), 315−320.
(27) Jackson, P. A.; Widen, J. C.; Harki, D. A.; Brummond, K. M. Covalent Modifiers: A Chemical Perspective on the Reactivity of α,β-Unsaturated Carbonyls with Thiols via Hetero-Michael Addition Reactions. *J. Med. Chem.* **2017**, *60* (3), 839−885.
(28) Robers, M. B.; Dart, M. L.; Woodroofe, C. C.; Zimprich, C. A.; Kirkland, T. A.; Machleidt, T.; Kupcho, K. R.; Levin, S.; Hartnett, J. R.; Zimmerman, K.; Niles, A. L.; Ohana, R. F.; Daniels, D. L.; Slater, M.; Wood, M. G.; Cong, M.; Cheng, Y.-Q.; Wood, K. V. Target Engagement and Drug Residence Time Can Be Observed in Living Cells with BRET. *Nat. Commun.* **2015**, *6* (1), 10091.
(29) Steiner, J. P.; Hamilton, G. S.; Ross, D. T.; Valentine, H. L.; Guo, H.; Connolly, M. A.; Liang, S.; Ramsey, C.; Li, J. H. J.; Huang, W.; Howorth, P.; Soni, R.; Fuller, M.; Sauer, H.; Nowotnik, A. C.; Suzdak, P. D. Neurotrophic Immunophilin Ligands Stimulate Structural and Functional Recovery in Neurodegenerative Animal Models. *Proc. Natl. Acad. Sci. U. S. A.* **1997**, *94* (5), 2019−2024.
(30) Harper, S.; Bilsland, J.; Young, L.; Bristow, L.; Boyce, S.; Mason, G.; Rigby, M.; Hewson, L.; Smith, D.; O'Donnell, R.; O'Connor, D.; Hill, R. G.; Evans, D.; Swain, C.; Williams, B.; Hefti, F. Analysis of the Neurotrophic Effects of GPI-1046 on Neuron Survival and Regeneration in Culture and in Vivo. *Neuroscience* **1999**, *88* (1), 257−267.

https://dx.doi.org/10.1021/acsmedchemlett.0c00272
ACS Med. Chem. Lett. 2020, 11, 2131−2138